

# Gravity-driven flows in porous layers

By HERBERT E. HUPPERT AND ANDREW W. WOODS

Institute of Theoretical Geophysics, Department of Applied Mathematics and Theoretical Physics, Silver Street, Cambridge, CB3 9EW, UK

(Received 18 May 1994)

The motion of instantaneous and maintained releases of buoyant fluid through shallow permeable layers of large horizontal extent is described by a nonlinear advection–diffusion equation. This equation admits similarity solutions which describe the release of one fluid into a horizontal porous layer initially saturated with a second immiscible fluid of different density. Asymptotically, a finite volume of fluid spreads as  $t^{1/3}$ . On an inclined surface, in a layer of uniform permeability, a finite volume of fluid propagates steadily upslope under gravity, and spreads diffusively owing to the gravitational acceleration normal to the boundary, as on a horizontal boundary. However, if the permeability varies in this cross-slope direction, then, in the moving frame, the spreading of the current eventually becomes dominated by the variation in speed with depth, and the current length increases as  $t^{1/2}$ . Shocks develop either at the leading or trailing edge of the flows depending upon whether the permeability increases or decreases away from the sloping boundary. Finally we consider the transient and steady exchange of fluids of different densities between reservoirs connected by a shallow long porous channel. Similarity solutions in a steadily migrating frame describe the initial stages of the exchange process. In the final steady state, there is a continuum of possible solutions, which may include flow in either one or both layers of fluid. The maximal exchange flow between the reservoirs involves motion in one layer only. We confirm some of our analysis with analogue laboratory experiments using a Hele-Shaw cell.

---

## 1. Introduction

The motion of water or other fluids through porous layers plays an important role in a wide variety of settings. One situation that has begun to receive considerable attention is the large-scale motion of fluids in the upper surface of the Earth. Sedimentary basins and fractured magmatic intrusions may support a significant flux of ground water. The dissolution and precipitation that may result from the motion of such ground water is central to our understanding of the chemical alteration which may occur in rocks and sediment layers thousands of years after their formation (Wood & Hewitt 1982; Phillips 1991). In particular, if an aqueous solution of one chemical composition invades the pore spaces of a rock which is in equilibrium with an aqueous solution of different composition, then a reaction may ensue, which alters the rock chemistry. In many cases the rate of reaction is limited by the gravitational exchange of fluid (Phillips 1991).

In the environmental context, waste fluid containing contaminants may spread through the water table. If the density of this fluid is different from that of the surrounding ground water, then the contaminant may propagate as a gravity current through the porous network of aquifers (Bear 1988; Turcotte & Schubert 1984). In the oil industry, the motion of lubricants around well bores is of considerable importance

for preservation of drills. As the buoyant lubricant rises around a well bore, it may reach an impermeable stratum and spread laterally along the boundary of the stratum as a gravity-driven flow (Dussan V. & Auzerais 1993).

A number of aspects of gravity-driven flows in porous rocks have been well studied (Bear 1988), and an overview of some of the geologically important problems is presented by Turcotte & Schubert (1984). If the two fluids mix very slowly, then the fluids retain their identity for a considerable time and many of the resulting gravitationally driven flows admit similarity solutions, some of which, to our knowledge, have not been previously described. In particular, we consider here the short- and long-term asymptotic evolution of finite releases of fluid as they propagate under gravity along horizontal and sloping layers saturated with a second immiscible fluid. In our analysis we identify important differences between motion in a layer of uniform permeability and one in which the permeability changes in the direction normal to the boundary. We present travelling similarity solutions for finite releases of material which indicate how the short- and long-term spreading of the currents is affected. We also consider the exchange of fluids of different densities between two reservoirs of different initial pressure which are connected by a shallow porous channel of large lateral extent. In this two-layer generalization of the theory we again find travelling similarity solutions for the initial adjustment of the current, and describe a range of steady-state exchange flows, including the maximal exchange flow.

## 2. The governing equations

Consider the motion of a two-dimensional current of small aspect ratio (depth/length)  $\epsilon \ll 1$  propagating along a sloping boundary inclined at an angle  $\theta$  to the horizontal. If the current has Darcy velocity  $\mathbf{u} = (u, v)$  then the equation for conservation of mass

$$\nabla \cdot \mathbf{u} = 0 \quad (2.1)$$

indicates that  $v \sim \epsilon u$ . Thus to leading order the motion is parallel and along the slope. The equation of motion for the current is given by Darcy's law (Bear 1988; Phillips 1991; Dullien 1992) as

$$\mathbf{u} = -\frac{k(\phi)}{\mu} [\nabla P + \rho g(-\sin \theta, \cos \theta)], \quad (2.2)$$

where  $\mu$  is the dynamic viscosity,  $k$  is the permeability, which is a function of the void fraction  $\phi$ ,  $g$  is the gravitational acceleration and  $\rho$  is the constant uniform density of the current. The current occupies the region  $0 < y < h(x, t)$ ,  $0 < x < L(t)$ , and consists of fluid whose density is  $\Delta\rho$  in excess of that of the original fluid in the layer (figure 1). We assume that the upper layer is sufficiently deep that any secondary motion induced by the current is negligible. The pressure within the layer is hydrostatic and given by

$$P(x, y, t) = -g \cos \theta \Delta\rho y + p(x, t) \quad (2.3)$$

in terms of the hydrostatic pressure on the slope

$$p(x, t) = (\rho - \Delta\rho) g x \sin \theta + \Delta\rho g h(x, t) \cos \theta + P_1, \quad (2.4)$$

where  $P_1$  is a constant. We deduce from (2.2) that the alongslope motion in the current is given by

$$u(x, y, t) = -\frac{k(\phi)}{\mu} \Delta\rho g \left( \frac{\partial h}{\partial x} \cos \theta - \sin \theta \right). \quad (2.5)$$

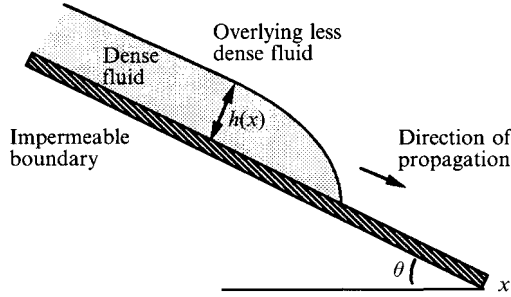


FIGURE 1. Schematic of a gravity current propagating in a tilted porous layer.

The local equation for the conservation of mass in the current is given by

$$\frac{\partial}{\partial x} \left[ \int_0^{h(x,t)} u(x,y,t) dy \right] = -\phi(h) \frac{\partial h}{\partial t}. \quad (2.6)$$

By combining (2.5) and (2.6), we obtain the local equation describing the evolution of the current

$$\frac{g\Delta\rho}{\mu} \frac{\partial}{\partial x} \left[ \left( \frac{\partial h}{\partial x} \cos \theta - \sin \theta \right) \int_0^{h(x,t)} k(\phi) dy \right] = \phi(h) \frac{\partial h}{\partial t}. \quad (2.7)$$

The equation describing the global conservation of mass is

$$\int_0^{L(t)} dx \left( \int_0^{h(x,t)} \phi(y) dy \right) = \int_0^t q(t') dt' = Q(t), \quad (2.8 a, b)$$

where  $q(t)$  is the volume flux at the source and  $Q(t)$  the total volume at time  $t$ . Typically, the permeability may be related to the porosity by a relationship of the form

$$k(\phi) = k_0 \phi^n. \quad (2.9)$$

In many natural rocks it has been found that  $2 \leq n \leq 3$  (Phillips 1991; Dullien 1992). If we assume that the porosity varies linearly in the direction normal to the boundary, so that

$$\phi = \phi_0 + \phi_1 y$$

with  $\phi_0$  non-zero, (2.7) reduces to

$$R \frac{\partial}{\partial x} \left[ \left( \left( 1 + \frac{\phi_1 h}{\phi_0} \right)^{n+1} - 1 \right) \left( \frac{\partial h}{\partial x} \cos \theta - \sin \theta \right) \right] = \left( 1 + \frac{\phi_1 h}{\phi_0} \right) \frac{\partial h}{\partial t}, \quad (2.10)$$

where  $R = \phi_0^n \Delta\rho g k_0 / [\phi_1 (n+1) \mu]$  and the global conservation of mass may be expressed as

$$\int_0^{L(t)} \frac{(\phi_0 + \phi_1 h)^2 - \phi_0^2}{2\phi_1} dx = Q(t). \quad (2.11)$$

As the current propagates alongslope and spread,  $h$  steadily decreases and the ratio  $\phi_1 h / \phi_0$  typically becomes very small, indicating that the variation in porosity across the current is small. In this limit (2.10) and (2.11) have the approximate forms

$$S \frac{\partial}{\partial x} \left[ (h + n\delta h^2) \left( \frac{\partial h}{\partial x} \cos \theta - \sin \theta \right) \right] = (1 + 2\delta h) \frac{\partial h}{\partial t} \quad (2.12)$$

and

$$\phi_0 \int_0^{L(t)} h(1 + \delta h) dx = Q(t), \quad (2.13)$$

where  $\delta = \frac{1}{2}\phi_1/\phi_0$  and  $S = \phi_0^{n-1} \Delta \rho g k_0 / \mu$ . To lowest order  $\delta$  may be set equal to zero, but additional effects emerge at the next order and so we retain all the terms displayed in (2.12) and (2.13). In the next two sections we obtain solutions to this coupled system of equations.

We note that many of the flows described by the above model are ultimately influenced by diffusion or mixing of the density-producing agent between the input fluid and the ambient fluid, leading to buoyancy-dispersion type flows (e.g. Erdogan & Chatwin 1969). The following analyses strictly only apply until such a time.

### 3. Horizontal boundaries

The self-similar propagation of gravity currents along a horizontal boundary represents an important limit for the propagation of currents along inclined boundaries. On a horizontal boundary,  $\theta = 0$ , and (2.12) reduces to the simpler form

$$S \frac{\partial}{\partial x} \left[ h(1 + n\delta h) \frac{\partial h}{\partial x} \right] = (1 + 2\delta h) \frac{\partial h}{\partial t}. \quad (3.1)$$

If the fluid is supplied at a rate  $q(t) = q_0 t^{-1/2}$ , then  $Q = 2q_0 t^{1/2}$  and in this somewhat special case the system of equations admits similarity solutions  $h = Hf(\eta)$  and  $L = \lambda(Dt)^{1/2}$ , where  $\eta = x/(Dt)^{1/2}$ ,  $H = (q_0^2/S)^{1/3}$  and  $D = (Sq_0)^{2/3}$ . In these similarity solutions,  $f$  is determined by the equation

$$-2 \frac{d}{d\eta} \left( f(1 + n\delta Hf) \frac{df}{d\eta} \right) = \eta \frac{df}{d\eta} (1 + 2\delta Hf) \quad (3.2)$$

together with boundary conditions

$$f(\lambda) = 0 \quad \text{and} \quad \phi_0 \int_0^\lambda f(1 + \delta fH) d\eta = 2. \quad (3.3a, b)$$

This description in terms of similarity variables extends the results of Bear (1988), who discussed the case of a layer of uniform permeability.

To proceed further we consider the limit  $\delta \rightarrow 0$ , which corresponds to a layer of uniform permeability and porosity, and in which limit a much wider class of similarity solutions exist. Equations (3.1) and (2.13) then reduce to the simpler forms

$$S \frac{\partial}{\partial x} \left( h \frac{\partial h}{\partial x} \right) = \frac{\partial h}{\partial t}, \quad (3.4)$$

$$\phi_0 \int_0^{L(t)} h dx = Q(t). \quad (3.5)$$

If  $Q(t) = Q_0 t^\gamma$  equations (3.4) and (3.5) are satisfied by a family of similarity solutions of the form  $h(x, t) = H_\gamma (D_\gamma t)^\alpha f_\gamma(\xi)$  and  $L = \lambda H_\gamma (D_\gamma t)^\beta$ , where  $\xi = x/H_\gamma (D_\gamma t)^\beta$ ,  $H_\gamma = (Q_0/S^\gamma)^{1/(2-\gamma)}$ ,  $D_\gamma = (S^2/Q_0)^{1/(2-\gamma)}$ ,  $\alpha = (2\gamma - 1)/3$ ,  $\beta = (\gamma + 1)/3$  and  $f_\gamma(\xi)$  is determined by the equation

$$3 \frac{d}{d\xi} \left( f_\gamma \frac{df_\gamma}{d\xi} \right) = (2\gamma - 1) f_\gamma - (\gamma + 1) \xi \frac{df_\gamma}{d\xi} \quad (3.6a)$$

together with the boundary conditions

$$f_\gamma(\lambda) = 0 \quad \text{and} \quad \phi_0 \int_0^\lambda f_\gamma(\xi) d\xi = 1. \quad (3.6b, c)$$

For the case  $\gamma = 0$ , corresponding to a finite release of fluid  $Q_0$ , (3.6) can be integrated analytically to obtain the shape of the interface in the form of the parabola

$$f_0(\xi) = (\xi_0^2 - \xi^2)/6, \quad (3.7)$$

where  $\xi_0 = (9/\phi_0)^{1/3}$ . In this case, the current thickness decreases as  $(St/Q_0^2)^{-1/3}$  and the length of the current increases as  $(Q_0 St)^{1/3}$ .

### Experimental Investigation

In order to investigate the validity of our theoretical approach, we have carried out a series of laboratory experiments using a thin Hele-Shaw cell, arranged so that the plane normal to the plates is horizontal. When a viscous fluid flows under gravity between two vertical closely spaced plates, sidewall friction is dominant and is analogous to the local friction in a porous layer as given by Darcy's Law. The dynamical equation describing flow in a Hele-Shaw cell represents a balance between the viscous drag and the buoyancy force and leads to the velocity profile

$$u = -(12b^2\Delta\rho g/\mu) \partial h/\partial x, \quad (3.8)$$

where  $b$  is the width of the cell (cf. (2.5) with  $\theta \equiv 0$ ). Combining (3.8) with the local continuity equation, we obtain the governing differential equation (Huppert 1986)

$$R \frac{\partial}{\partial x} \left( h \frac{\partial h}{\partial x} \right) = \frac{\partial h}{\partial t}, \quad (3.9)$$

where  $R = \Delta\rho g b^2/12\mu$ , while the global conservation of mass has the form

$$\int_0^{L(t)} h dx = \int_0^t q dt' = Q(t). \quad (3.10)$$

These equations are identical in form to (3.4) and (3.5).

For the instantaneous release of a finite volume of fluid per unit width,  $V$ , in the Hele-Shaw cell the current propagates according to

$$L(t) = (9VRt)^{1/3} \quad (3.11)$$

and takes the shape

$$h = \frac{1}{6}(V^2/R)^{1/3} (\zeta_0^2 - \zeta^2) t^{-1/3}, \quad (3.12)$$

where  $\zeta = x/(VRt)^{1/3}$  and  $\zeta_0 = 9^{1/3}$ . In order to test the theory, a finite volume of glycerine was released into an (air-filled) Hele-Shaw cell, 1 cm wide, and the shape and location of the leading edge of the current were then monitored with time. The Bond number of the flow (Huppert 1982) was large, and so effects of surface tension at the interface between the air and the glycerine were unimportant. Figure 2 presents the measured shape of a glycerine current (crosses) and compares this to the shape predicted by (3.12) (solid line). The comparison was made 150 s after the release of the current, which initially had a rectangular cross-section of height 14 cm and length 9 cm. The agreement is seen to be quite good, especially given the experimental error in the measurement of the height of  $\pm 1.0$  mm. The leading edge of the actual current lags

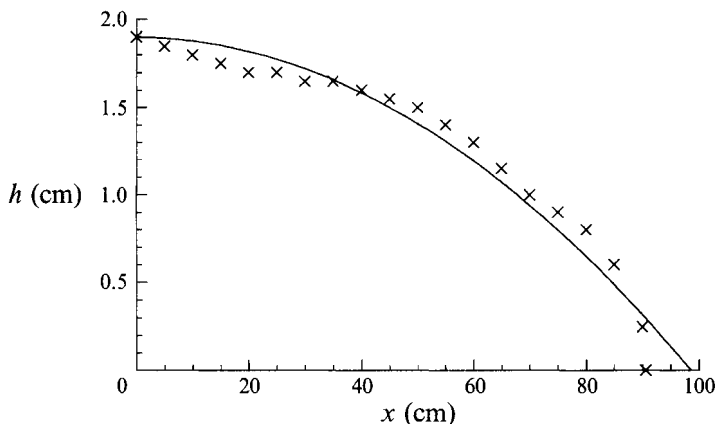


FIGURE 2. The experimentally measured shape of a current (crosses), of initial height 14 cm and length 9 cm, 150 s after release. The shape is compared with the theoretical prediction (solid curve, equation (3.12)). The glycerine in the experiment had a viscosity of  $7 \text{ cm}^2 \text{ s}^{-1}$ , and the plates of the Hele-Shaw cell were 1 cm apart. Some discrepancies develop near the leading edge of the current as a result of the increasing importance of the bottom friction near the nose.

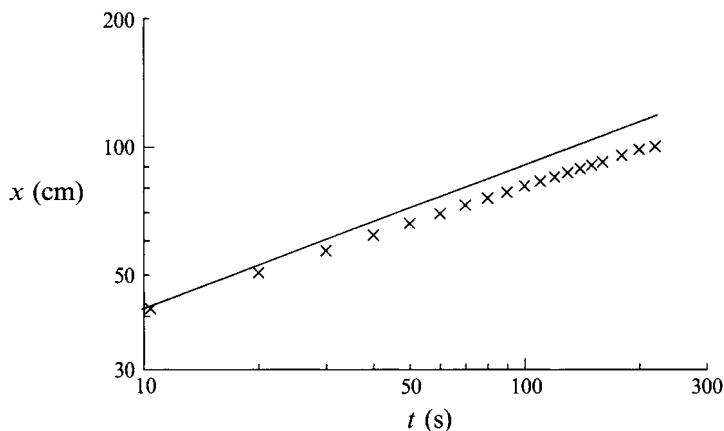


FIGURE 3. Position of the front of the current as a function of time as it propagates through an experimental Hele-Shaw cell. The experimental parameters are as in figure 2. The experimental results are compared with the theoretical prediction for the spreading rate given by equation (3.11).

behind the model prediction owing to the increasing role of the viscous drag from the base of the tank as the current thins. Figure 3 shows how the position of the leading edge of the current changes with time during an experiment (crosses) and as predicted by the theory (solid line). Initially the agreement is quite good, but with time the experimental current gradually begins to fall behind the theoretical prediction. Again this is due to the fact that as the length of the current increases and the height decreases, the current is additionally retarded at the base. This effect is not as pronounced for a gravity current driven by a constant flux, as is discussed in the next paragraph.

For the release of a constant flux of fluid per unit width,  $F$ , the length of the current is given by

$$L(t) = 1.48(FRt^2)^{1/3}, \quad (3.13)$$

where the constant of proportionality is obtained by numerical integration of (3.9) and

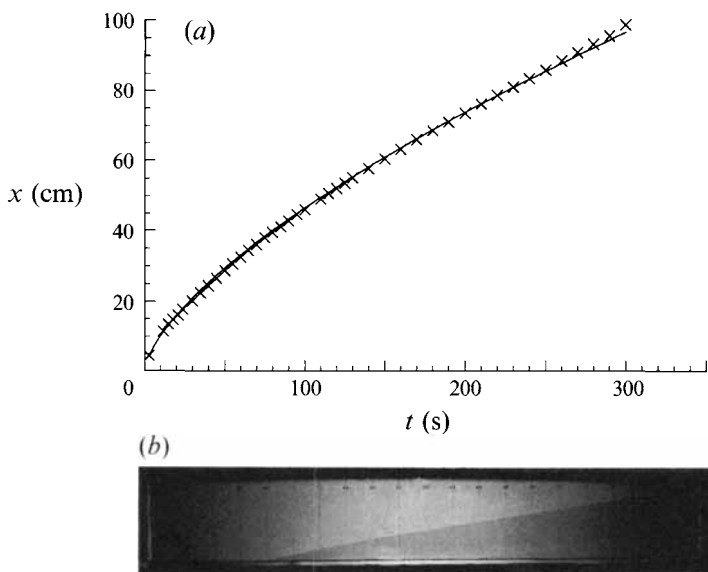


FIGURE 4. (a) Position of the front of a steady release of fluid as it propagates through an experimental Hele-Shaw cell as a function of time. The experimental results are compared with the theoretical spreading rate of equation (3.13). In this experiment, the plates of the Hele-Shaw cell were 0.45 cm apart, and the glycerine was supplied at the rate  $1 \text{ cm}^3 \text{ s}^{-1}$ . (b) Photograph showing the structure of a laboratory gravity current of glycerine supplied at a constant rate  $1 \text{ cm}^3 \text{ s}^{-1}$  to a Hele-Shaw cell of width 4.5 cm.

(3.10) expressed in appropriate similarity variables (Huppert 1986). Figure 4(a) shows that the theoretical relationship (3.13) is in excellent agreement with the data obtained from an experiment in which glycerine was injected into a Hele-Shaw cell, 4.5 mm wide, at a constant rate  $1 \text{ cm}^3 \text{ s}^{-1}$  (figure 4b).

## 4. Gravity currents on slopes

### 4.1. Solutions with constant permeability

On a sloping boundary, we return to the full equations for the current (2.12) and (2.13). In the limit of constant permeability  $\delta \rightarrow 0$ , and (2.12) reduces to

$$S \cos \theta \frac{\partial}{\partial x} \left[ h \frac{\partial h}{\partial x} \right] = S \sin \theta \frac{\partial h}{\partial x} + \frac{\partial h}{\partial t}. \quad (4.1)$$

For the release of a finite volume of fluid,  $Q_0$ , the motion consists of a steady propagation downslope driven by the alongslope component of gravity, combined with a slow diffusive spreading as a result of the cross-slope component of gravity. In the steadily moving frame,  $x = S \sin \theta t$ , we can adopt the second similarity solution of §3 with  $\gamma = 0$ , and write  $h$  in the form  $h = (Q_0^2 / St \cos \theta)^{1/3} f_0(\omega)$  where  $\omega = z / (Q_0 St \cos \theta)^{1/3}$  and  $z = x - St \sin \theta$ . In the moving frame the spreading due to the component of gravity normal to the boundary occurs at a rate proportional to  $t^{1/3}$ . Indeed, an initially symmetrical parcel of fluid propagating downslope has the self-similar form  $f_0(\omega) = (\omega_0^2 - \omega^2)/6$  for  $-\omega_0 < \omega < \omega_0$  where  $\omega_0 = (9/\phi_0)^{1/3}$ . If the initial length of the current is  $L_0$ , then it preserves its shape for times shorter than  $\tau = L_0^3 / Q_0 S \cos \theta$ , and simply propagates downslope at a speed  $S \sin \theta$ . For times longer than  $\tau$ , the current spreads out alongslope as a result of the component of gravity normal to the slope (figure 5).

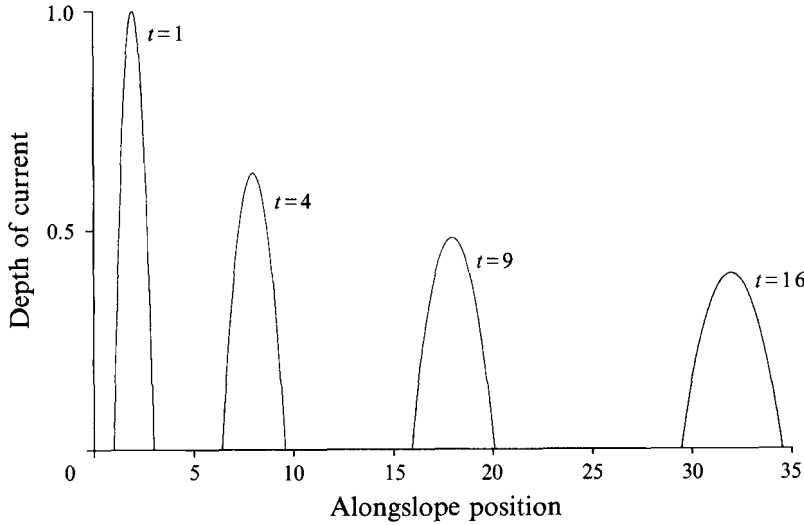


FIGURE 5. The theoretical evolution of a finite release of fluid down a slope as it slumps under gravity. The current position and shape is shown at various times after the initial release.

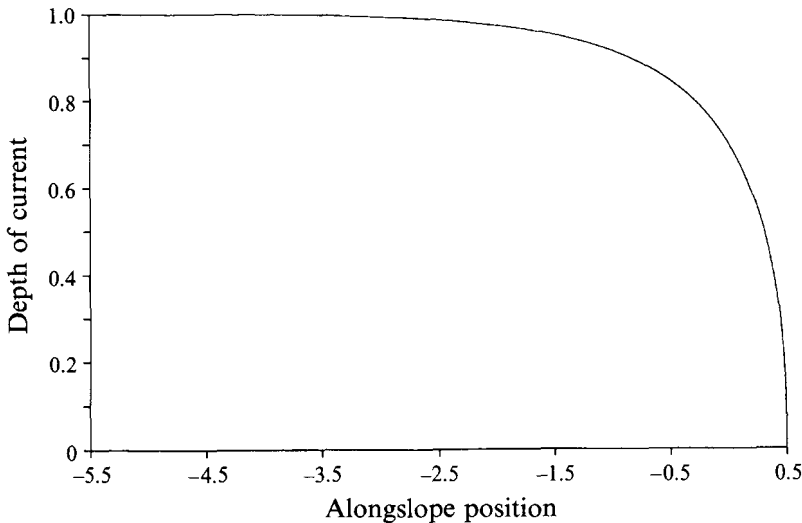


FIGURE 6. The structure of the boundary layer at the front of a uniform current propagating downslope in a uniform porous layer from a maintained source of fluid.

For a maintained release of fluid at a point  $x_0$ , with a fixed flux  $M$  say, to leading order the current propagates downslope with speed  $S \sin \theta$  and fixed depth  $h_0 = M / (S \sin \theta)$  except at the leading edge of the current. At the leading edge, the component of gravity normal to the slope allows a smooth adjustment of the current depth from  $h_0$  far upstream to zero. Transforming coordinates to the moving frame of the front,  $x = S \sin \theta t$ , and writing  $h = h_0[1 - g(z, t)]$  we find that  $g$  satisfies the diffusion equation

$$\frac{\partial g}{\partial t} = M \cot \theta \frac{\partial}{\partial z} \left( (1 - g) \frac{\partial g}{\partial z} \right). \quad (4.2)$$

This equation admits similarity solutions  $g(\sigma)$  in terms of the similarity variable  $\sigma = z / (M \cot \theta t)^{1/2}$  with boundary conditions that  $g \rightarrow 0$  as  $\sigma \rightarrow -\infty$  and  $\int_{-\infty}^{\lambda} g \, d\sigma = 0$

where  $g(\lambda) = 1$ . The full numerical solution (figure 6) identifies that  $\lambda = 0.5$ . This boundary layer at the head of the current therefore grows in length as  $(M \cot \theta t)^{1/2}$  and has the form shown in figure 6.

#### 4.2. Solutions with variable permeability

Consider the release of a finite mass of fluid,  $Q_0$ . Then the equation governing the motion along the slope has the approximate form

$$S \cos \theta \frac{\partial}{\partial x} \left[ (h + n\delta h^2) \frac{\partial h}{\partial x} \right] = S \sin \theta (1 + 2n\delta h) \frac{\partial h}{\partial x} + (1 + 2\delta h) \frac{\partial h}{\partial t}, \quad (4.3)$$

where we have neglected terms in powers of  $\delta^2$ . To leading order, the current propagates steadily along the slope, as if the layer were of uniform permeability. However, there is a slow evolution of the shape of the current owing to both the diffusive spreading of the current, which results from the component of gravity normal to the slope, and the steepening of the head of the current ( $\delta > 0$ ) owing to the variation of permeability normal to the slope and hence speed alongslope. These two processes are important at different stages in the history of the current, and may be understood by changing coordinates to the steadily propagating frame  $z = x - St \sin \theta$ . In this frame, the governing equation has the leading-order form

$$S \cos \theta \frac{\partial}{\partial z} \left( h \frac{\partial h}{\partial z} \right) = 2Sn\delta \sin \theta h \frac{\partial h}{\partial z} + \frac{\partial h}{\partial t}, \quad (4.4)$$

where  $h = h(z, t)$ . The term on the left-hand side denotes the diffusive influence of the component of gravity normal to the slope acting on the current, while the first term on the right-hand side denotes the motion produced by the alongslope component of gravity as a result of the increase in permeability with position normal to the slope.

At both early and long times, the motion of the finite release of fluid is described by self-similar solutions of the form  $h = H(Dt)^\alpha f_0(\eta)$  where  $\eta = z/H(Dt)^\beta$  and  $\int_0^\lambda f_0 d\eta = 1/\phi_0$ , and  $H$  and  $D$  are defined below. The two solutions are found by balancing either (i) the alongslope dispersion of the current which results from the variation in permeability normal to the slope or (ii) the diffusive slumping of the current due to the gravitational acceleration normal to the slope with the time derivative. The critical time at which these solutions predict the same thickness of the current, and hence at which the dominant physical balance changes is  $t^* = Q_0^2/(2Sn^3\delta^3 \tan^2 \theta \sin \theta)$ .

At short times,  $t \ll t^*$ , the dominant motion relative to the moving frame consists of the gravitational slumping of the current caused by the component of gravity normal to the slope. In this case,  $\alpha = -\beta = -\frac{1}{3}$ ,  $H = Q_0^{1/2}$  and  $D = S \cos \theta / Q_0^{1/2}$  and we recover the solution described in §4.1.

However, at longer times,  $t \gg t^*$ , the tendency for the current to steepen at its leading edge ( $\delta > 0$ ) owing to the increase in velocity with depth, becomes dominant and the component of gravity normal to the slope becomes negligible. The long-term asymptotic behaviour is described with  $\alpha = -\beta = -\frac{1}{2}$ ,  $H = Q_0^{1/2}$  and  $D = 2Sn\delta \sin \theta$ . Therefore, as  $t \rightarrow \infty$ ,  $h \sim Q_0^{1/2} (2Sn\delta t \sin \theta)^{-1/2} f_0(\eta)$  where

$$f_0 \frac{df_0}{d\eta} = \frac{1}{2} \frac{d(\eta f_0)}{d\eta}. \quad (4.5)$$

The steepening of the current which results from the increasing permeability with distance from the slope causes the current to spread out as  $(Q_0 S \sin \theta n \delta t)^{1/2}$ , with the current depth decreasing as  $(Q_0 S \sin \theta n \delta t)^{-1/2}$ . Integrating (4.5), we deduce that  $f_0 = \eta$

and that the current is confined to the interval  $0 < \eta < \eta_0 = (2/\phi_0)^{1/2}$ . At the front of the current there is a rapid adjustment from the maximum depth,  $\eta_0$ , to zero. This adjustment occurs in a region of width  $\eta_0/t^{1/2}$ . Introducing a boundary layer coordinate  $\zeta = (\eta_0 - \eta)(2Sn\delta \sin \theta t)^{1/2}$ , it may be shown that (4.3) has the leading-order form

$$h = \frac{Q_0^{1/2}}{(2Sn\delta \sin \theta t)^{1/2}} g(\zeta),$$

where

$$\Gamma \frac{d}{d\zeta} \left( g \frac{dg}{d\zeta} \right) = -g \frac{dg}{d\zeta} + \frac{\eta_0}{2} \frac{dg}{d\zeta} \quad (4.6)$$

in this boundary layer and  $\Gamma = \cot \theta / (2n\delta Q^{1/2})$ . The current therefore adjusts to zero depth at the leading edge ( $\delta > 0$ ) according to

$$g(\zeta) = \eta_0 \left( 1 - \exp \left( -\frac{\zeta}{2\Gamma} \right) \right). \quad (4.7)$$

It is worth noting that if  $\delta < 0$ , then the current tends to steepen at its tail, since this corresponds to a decrease in the permeability and flow rate with distance above the boundary. A similar analysis carries through in that case also. There is an interesting analogy between the above long-time solution and the long-time motion of a viscous current on a slope as described by Lister (1992). In the present case the effect of the variable permeability causing the alongslope dispersion is analogous to the dispersion which occurs in a viscous current as a result of the increase in flow rate with current thickness. However, an important difference arises from the absence of a no-slip condition in the present case. This allows the current to move downslope as a simple wave to leading order.

## 5. Exchange flows between adjacent reservoirs

### 5.1. The governing equations

A further problem of importance in geophysical and other contexts concerns the exchange of fluids of different densities between two reservoirs connected by a porous channel. Analysis of such flows involves a generalization of the previous theory to a two-layer system. Amongst other situations, this occurs in coral atolls as a result of tidal variations in the level of saline reservoirs and in sedimentary basins as a result of long-term climate changes (Byorlykke 1987). Such exchange flows may also have an important control upon the rate of mineral replacement reactions (e.g. Davis *et al.* 1985; Linz & Woods 1992).

We consider two reservoirs saturated with fluids of densities  $\rho$  and  $\rho - \Delta\rho$ , which become connected by a narrow long porous channel of porosity  $\phi$  at time  $t = 0$  (figure 7). The heavy fluid therefore passes under the light fluid. In a long narrow channel, to leading order the velocities in each layer are along channel, and if the channel is of uniform permeability the flow in each layer is uniform. Suppose the channel has depth  $H$ , the lower layer of dense fluid has depth  $h(x)$  and velocity  $u_1(x)$ , while the upper layer has velocity  $u_2(x)$ .

If the pressure on the lower boundary of the channel is  $p(x, t)$  then the pressure within the lower layer,  $0 < y < h(x, t)$ , is given by

$$P(x, y, t) = p(x, t) - \rho gy \quad (5.1)$$

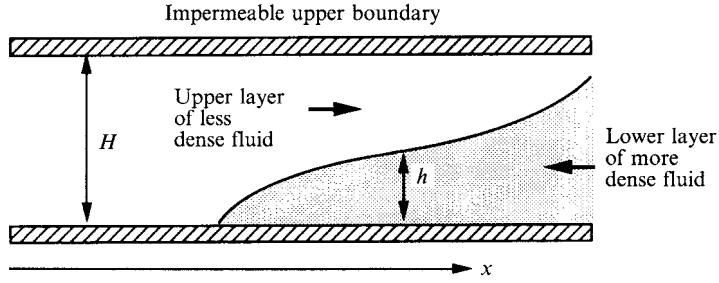


FIGURE 7. Schematic of the flow configuration for the exchange flow between two porous reservoirs containing fluids of different density and at different pressure.

and that in the upper layer,  $h(x, t) < y < H$ , is given by

$$P(x, y, t) = p(x, t) - \rho g y + \Delta \rho g [y - h(x, t)]. \quad (5.2)$$

The equation of motion in the lower layer is therefore

$$u_1 = -\frac{k}{\mu} \frac{\partial p}{\partial x}, \quad (5.3)$$

while that in the upper layer is

$$u_2 = -\frac{k}{\mu} \left( \frac{\partial p}{\partial x} - \Delta \rho g \frac{\partial h}{\partial x} \right) = u_1 + \frac{k \Delta \rho g}{\mu} \frac{\partial h}{\partial x}. \quad (5.4a, b)$$

Conservation of mass in the lower layer requires that

$$\phi \frac{\partial h}{\partial t} + \frac{\partial u_1 h}{\partial x} = 0 \quad (5.5)$$

while the total mass flux through the channel

$$Q = h u_1 + (H - h) u_2 \quad (5.6)$$

is independent of length along the channel. Combining (5.3), (5.4) and (5.6), we find that

$$u_1 = -\frac{k}{\mu} \frac{\partial p}{\partial x} = \frac{Q}{H} - \frac{k \Delta \rho g}{\mu H} (H - h) \frac{\partial h}{\partial x}, \quad (5.7a, b)$$

which when substituted into (5.5) yields

$$\frac{\partial \psi}{\partial t} + \frac{Q}{\phi H} \frac{\partial \psi}{\partial x} = A \frac{\partial}{\partial x} \left[ \frac{\partial \psi}{\partial x} (1 - \psi) \psi \right], \quad (5.8)$$

where  $\psi = h/H$  is the dimensionless depth of the lower layer and

$$A = k \Delta \rho g H / \mu \phi. \quad (5.9)$$

Integrating (5.7b) along the channel  $0 < x < L$  and rearranging the result, we find that

$$Q(t) = \frac{H A \phi}{L} \left( [\psi(L, t) - \frac{1}{2} \psi^2(L, t)] - [\psi(0, t) - \frac{1}{2} \psi^2(0, t)] - \frac{\Delta p}{\Delta \rho g H} \right), \quad (5.10)$$

which relates the flux  $Q$  to the difference in pressure between the two reservoirs at the height of the lower boundary,  $\Delta p$ .

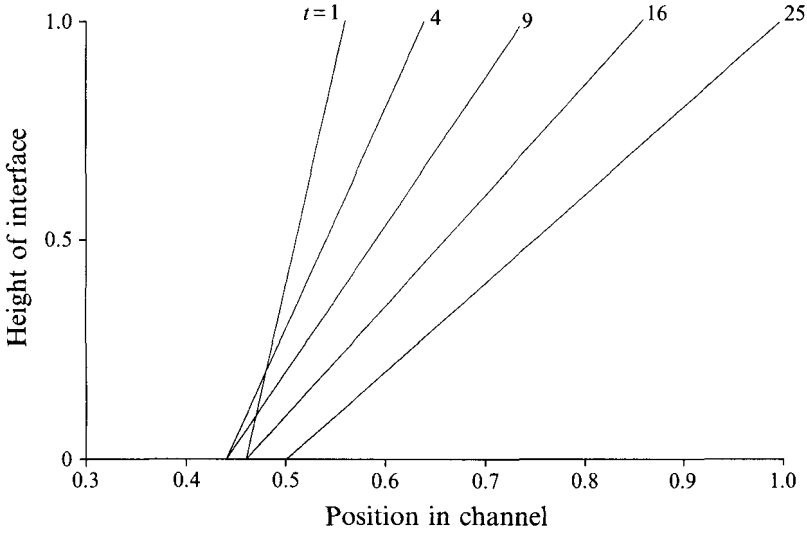


FIGURE 8. The variation in the location of the interface between the two fluid layers as a function of time showing that initially the slumping under gravity dominates, but that subsequently the pressure-driven flow can dominate the motion.

### 5.2. The self-similar transient flow

During the initial exchange of fluid between the reservoirs, the interface position evolves with time as a result of both the overall pressure gradient which drives a net flow, and also the density difference which drives a wedge of dense fluid along the bottom boundary and a wedge of light fluid along the top boundary. In the moving frame described by  $z = x - Qt/\phi H$ , (5.8) becomes

$$\frac{\partial \psi}{\partial t} = A \frac{\partial}{\partial z} \left( \psi(1-\psi) \frac{\partial \psi}{\partial z} \right). \quad (5.11)$$

This equation admits a similarity solution of the form  $\psi = f_e(\zeta)$  with similarity variable  $\zeta = x/(At)^{1/2}$  in the region  $-\lambda < \zeta < \lambda$  which satisfies the boundary conditions  $f_e(\lambda) = 1$ ,  $f_e(-\lambda) = 0$  where  $f_e$  is given by the equation

$$-\zeta \frac{df_e}{d\zeta} = 2 \frac{d}{d\zeta} \left( f_e(1-f_e) \frac{df_e}{d\zeta} \right). \quad (5.12)$$

Equation (5.12) has a solution  $f_e(\zeta) = \frac{1}{2}(1 + \zeta)$  with eigenvalue  $\lambda = 1$ . This solution is valid until the fluid interface reaches one end of the channel, that is while both  $\psi(0, t) = 0$  and  $\psi(L, t) = 1$ . From (5.10),  $Q$  is constant during this time. In figure 8, we have plotted the position of the interface between the two fluid layers, relative to a stationary frame, as a function of time. It is seen that initially, the self-similar spreading under gravity dominates the motion and the two edges propagate in different directions. However, as the interface becomes more horizontal, the background pressure field begins to dominate the motion, and the whole interface propagates in the direction of decreasing pressure. Once the interface between the two layers reaches either end of the channel, the above solution breaks down and the flow adjusts to a steady state. Bear (1988) reported a numerical solution of equation (5.12) which indicated that the current spread as  $t^{1/2}$ . However, we are unaware of any previous analytical solutions for this flow and it is an open question as to whether the nonlinear eigenvalue problem (5.12) above has any other solutions.

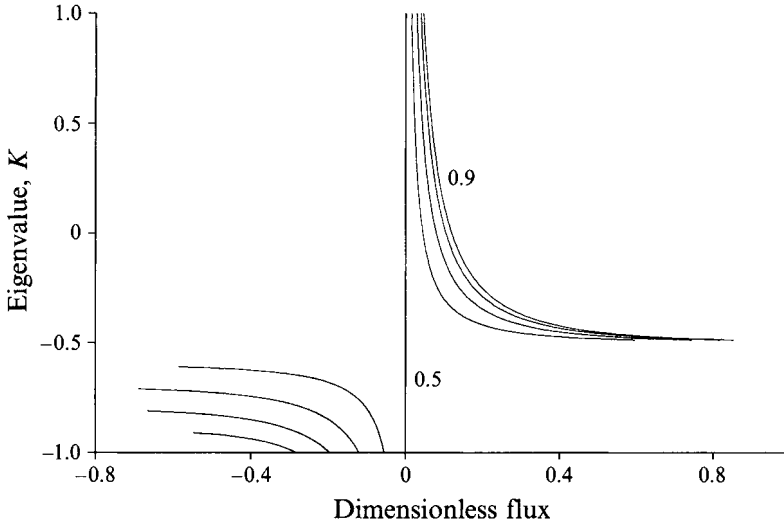


FIGURE 9. The variation of the eigenvalue  $K$  as a function of the dimensionless flux  $Q^*$ . Curves are shown for  $\psi(0) = 0.5$  and several values of  $\psi(1) = 0.5, 0.6, 0.7, 0.8$  and  $0.9$ ; the outer curves are labelled  $0.5$  and  $0.9$ . Note the asymmetry in the value of the eigenvalue as  $Q^*$  changes sign and the applied pressure gradient acts with or against the density gradient.

### 5.3. Steady-state exchange flows

Eventually, the initial transient exchange flows will establish a steady-state solution. Equation (5.10) is particularly instructive in understanding the range of possible steady solutions. In particular, the function  $(\psi - \frac{1}{2}\psi^2)$  ranges in value from  $0$  to  $\frac{1}{2}$  as  $\psi$  ranges from  $0$  to  $1$ . Therefore the maximum net flux  $Q$  which can be exchanged between the reservoirs is given in dimensionless form by

$$Q^* = \frac{1}{2} + |\Delta p^*|, \quad (5.13)$$

where  $\Delta p^* = \Delta p / \Delta \rho g H$  and  $Q^* = QL / HA \phi$ . This solution corresponds to the case in which the interface depth ranges from  $0$  to  $1$  across the channel. The equation for the shape of the interface may be found from (5.7). There are two types of solution, namely those in which there is flow in both layers with fluid being exchanged from each reservoir to the other, and those in which there is only flow from one reservoir to the other.

Denoting the dimensionless distance along the channel by  $\hat{x} = x/L$ , we obtain the steady version of (5.8) in the form

$$\psi(1 - \psi) \frac{d\psi}{d\hat{x}} = Q^*(\psi + K), \quad (5.14)$$

where  $K$  is a constant and here  $\psi = \psi(\hat{x})$ . In the case  $0 < \psi(0), \psi(1) < 1$ , corresponding to flow in both directions, (5.14) has solution

$$\begin{aligned} (\psi(\hat{x}) - \frac{1}{2}\psi(\hat{x})^2) - (\psi(0) - \frac{1}{2}\psi(0)^2) + K(\psi(\hat{x}) - \psi(0)) \\ - K(1 + K) \log \left( \frac{\psi(\hat{x}) + K}{\psi(0) + K} \right) = Q^* \hat{x}, \end{aligned} \quad (5.15)$$

where  $K$  is determined implicitly from (5.15) in terms of  $\psi(0)$  and  $\psi(1)$ . For example, in figure 9 we show how  $K$  varies with  $Q^*$  for  $\psi(0) = 0.5$  and  $\psi(1) = 0.6, 0.7, 0.8$  and

0.9. This corresponds to the case in which the applied pressure  $\Delta p$  is smaller than the change in the gravitational head  $\Delta\rho gH$ . Otherwise steady flow is only possible in one of the fluid layers.

If there is only exchange of fluid in one direction, then either  $\psi = 0$  in some region  $0 < \hat{x} < \hat{x}_1$  or  $\psi = 1$  in some region  $\hat{x}_2 < \hat{x} < 1$ . In the case  $\psi = 0$  in the region  $0 < \hat{x} < \hat{x}_1$ , the upper less-dense layer of fluid is driven through the channel. In order that there is no flow in the lower layer,  $K = 0$  (equation (5.14)). Therefore the interface has the profile given implicitly by

$$\psi - \frac{1}{2}\psi^2 = Q^*(\hat{x} - \hat{x}_1). \quad (5.16)$$

If we write  $\mathfrak{I} = \psi(1) - \frac{1}{2}\psi^2(1) > 0$  then combining (5.10) and (5.16) evaluated at  $\hat{x} = 1$ , we deduce that

$$Q^* = -\Delta p^*/\hat{x}_1 \quad \text{and} \quad \mathfrak{I} = -\Delta p^*(1 - \hat{x}_1)/\hat{x}_1. \quad (5.17a, b)$$

For a given value of  $\Delta p^*$  and  $\mathfrak{I}$ , we find that  $\hat{x}_1$  satisfies the relation  $\hat{x}_1 = -\Delta p^*/(\mathfrak{I} - \Delta p^*)$ . Since  $0 < \hat{x}_1 < 1$ , it follows that such solutions are only possible if  $\Delta p^* < 0$ . For given pressure difference  $\Delta p^*$ , the maximal flux occurs at the minimum value of  $\hat{x}_1$  (equation (5.17a)). This occurs when  $\mathfrak{I} = 0.5$  and is given by  $\hat{x}_1 = -2\Delta p^*/(1 - 2\Delta p^*)$ . The maximal flow rate,  $0.5 - \Delta p^*$ , is achieved when the fluid in the moving layer releases all the available potential energy associated with the fluid as it enters the channel.

Similarly, if the pressure gradient in the channel acts to drive the dense lower layer along the channel,  $\Delta p^* > 0$ , a stagnant layer of upper fluid can penetrate some distance into the channel,  $0 < \hat{x} < \hat{x}_2$  say, such that  $\psi(\hat{x}) = 1$  for  $\hat{x} > \hat{x}_2$ . In this case, in order that there is no flow in the upper layer,  $K = -1$ , and the shape of the interface is given by

$$\psi^2(\hat{x}) = 1 - 2Q^*(\hat{x} - \hat{x}_2) \quad (5.18)$$

for  $\hat{x} < \hat{x}_2$  and the maximal flow rate,  $0.5 + \Delta p^*$ , is achieved when the length of the intrusion of light fluid is  $2\Delta p^*/(1 + 2\Delta p^*)$ .

The selection of either the maximal or sub-maximal exchange flows depends upon the boundary conditions imposed at each end of the flow channel.

## 6. Conclusions

In this contribution we have developed a series of solutions to describe a number of gravity-driven flows in porous media. In §3, we presented a series of similarity solutions to describe the motion of instantaneous and maintained releases of dense fluid along a horizontal one-dimensional channel. Our solution approach may be readily extended to the case of axisymmetric geometry. We confirmed our theoretical predictions with a series of analogue laboratory experiments using a Hele-Shaw cell in which we examined currents produced from both an instantaneous and a continuous release of fluid. In §4, we discussed the different situation in which the flow propagates along a sloping channel. In this case, we showed that if the porosity increases or decreases with distance from the boundary, then, in the long-time asymptotic limit, a discrete release of fluid will tend to generate a discontinuity at the nose or tail of the flow respectively. In §5, we discussed both the initial transient and final steady-state flows which develop when a flow channel between two reservoirs of different density and pressure is opened. The transient exchange flow involves the self-similar motion of both fluids relative to a steadily migrating frame. In steady state there is a maximal exchange flow, involving motion in only one of the fluid layers, with a stagnant wedge of the other fluid layer

penetrating partially into the channel. If the pressure difference across the channel is sufficiently small, then fluid may be exchanged in both directions, at a sub-maximal flow rate.

We thank Mark Hallworth for assistance with the laboratory experiments. A. W. W. was supported by the 1993 WHOI GFD Summer School during the write-up of this work. The work of both H. E. H. and A. W. W. is supported by grants from the Natural Environment Research Council.

#### REFERENCES

- BEAR, J. 1988 *Dynamics of Fluids in Porous Media*. Dover.
- BYORLYKKE, K. 1989 *Sedimentology and Petroleum Geology*. Springer.
- DAVIES, S. H., ROSENBLATT, S., WOOD, J. R. & HEWITT, T. A. 1985 Convective fluid flow and diagenetic patterns in domed sheets. *Am. J. Sci.* **285**, 207–223.
- DULLIEN, F. A. L. 1992 *Porous Media – Fluid Transport and Pore Structure*. Academic.
- DUSSAN, V., E. B. & AUZERAIS, F. M. 1993 Buoyancy-induced flow in porous media generated near a drilled oil well. Part 1. The accumulation of filtrate at a horizontal impermeable boundary. *J. Fluid Mech.* **254**, 283–311.
- ERDOGAN, M. E. & CHATWIN, D. C. 1967 The effects of curvature and buoyancy on the laminar dispersion of solute in a horizontal tube. *J. Fluid Mech.* **29**, 465–484.
- HUPPERT, H. E. 1982 The propagation of two-dimensional and axisymmetric viscous gravity currents over a rigid horizontal surface. *J. Fluid Mech.* **121**, 43–58.
- HUPPERT, H. E. 1986 The intrusion of fluid mechanics into geology. *J. Fluid Mech.* **173**, 557–594.
- LINZ, S. J. & WOODS, A. W. 1992 Natural convection, Taylor dispersion, and diagenesis in a tilted porous layer. *Phys. Rev.* **46**, 4869–4878.
- LISTER, J. R. 1992 Viscous gravity currents downslope. *J. Fluid Mech.* **242**, 631–652.
- PHILLIPS, O. M. 1991 *Flow and Reactions in Permeable Rocks*. Cambridge University Press.
- TURCOTTE, D. L. & SCHUBERT, G. 1984 *Geodynamics*. John Wiley.
- WOOD, J. R. & HEWITT, T. A. 1982 Fluid convection and mass transport in porous limestones: A theoretical model. *Geochim. Cosmochim. Acta* **46**, 1707–1713.